Physica A 388 (2009) 2149–2156

Contents lists available at ScienceDirect

Physica A

journal homepage: www.elsevier.com/locate/physa

Drift velocity in the necklace model for reptation in a two-dimensional square lattice

G.R. Terranova [a], H.O. Mártin [a], C.M. Aldao [b,*]

[a] Departamento de Física, Facultad de Ciencias Exactas y Naturales, Universidad Nacional de Mar del Plata, Deán Funes 3350, B7602AYL Mar del Plata, Argentina

[b] Instituto de Investigaciones en Ciencia y Tecnología de Materiales (INTEMA), Universidad Nacional de Mar del Plata-CONICET, Juan B. Justo 4302, B7608FDQ Mar del Plata, Argentina

ARTICLE INFO

Article history:
Received 25 July 2008
Received in revised form 27 January 2009
Available online 13 February 2009

PACS:
05.40.-a
83.10.Kn
66.10.Cb

Keywords:
Monte Carlo simulations
Reptation
Necklace model
Drift

ABSTRACT

We report the chain dynamics in the necklace model that mimics the reptation of a chain of N particles in a two-dimensional square lattice. We focus on the drift velocity under an applied static field. The characteristics of the model allow us to determine the effects of the forces on the chains and the resulting mechanisms that affect the drift velocity. Results obtained through Monte Carlo simulations were analyzed and discussed and distinct regimes as a function of the force strength and N were identified. We found that for small total applied forces, the drift velocity scales as $1/N$. When the applied force to every particle is small but the total applied force is not, the tube deforms in such a way that the drift velocity does not depend on N. Large forces, applied to every particle, can straight chains such that the distance between the chain ends increases faster than the number of particles. Also, large forces can deform the chain within the tube what is directly related to a decrease of the drift velocity.

1. Introduction

The idea that the motion of entangled polymer chains takes place by "reptation" was introduced by de Gennes years ago [1]. He chose the word reptation because it describes the motion much like that of a snake moving in a contorted roadway formed by the surrounding polymer molecules. The reptation mechanism describes the dynamics of entangled polymer melts and also the motion of DNA molecules in gel electrophoresis. In both cases a long linear and flexible polymer moves in a medium of dense obstacles that confine its motion to a one-dimensional diffusion along a tube [2–4].

The first discretized model to analyze a chain dynamics under reptation was introduced by Rubinstein more than twenty years ago [5]. The repton model was then extended to two dimensions by Duke to adapt it to electrophoresis of DNA chains in a gel [6,7]. The gel was pictured by Duke as a square lattice of cells and the DNA molecule was considered to be a flexible repton chain that moves from cell to cell. Later, the necklace model that is slightly different from the repton model was introduced [8,9]. At odds with the Duke model, in the necklace model consecutive beads cannot occupy the same site. Also, the necklace model is more flexible regarding the jumping probability of beads at the ends of the chain relative to those of the central beads, allowing the study of cases that could not be addressed before.

We recently studied the reptation of a chain in a square lattice extending to two dimensions the necklace model [10]. Analytical approximations for the diffusion coefficient of the center of mass of the chain, for all values of N, were proposed. In this work, we focus on the drift velocity due to a static field. We found that the application of an external field can deeply affect the reptation motion and induce a rich non trivial phenomenology. We specifically study how the applied forces

* Corresponding author. Tel.: +54 223 4816600; fax: +54 223 4810046.
E-mail address: cmaldao@mdp.edu.ar (C.M. Aldao).

0378-4371/$ – see front matter © 2009 Elsevier B.V. All rights reserved.
doi:10.1016/j.physa.2009.02.001

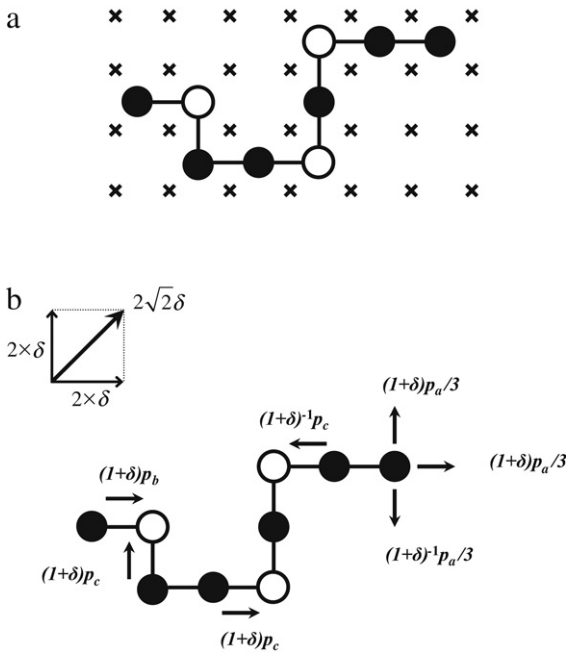

Fig. 1. Scheme representing the two-dimensional necklace model. (a) Chain in a gel or in a melt of others polymers chains. Filled circles represent particles of the chain, open circles holes, and crosses the gel or other fixed polymers that act as obstacles. (b) Jumping rates for end and middle particles when external forces are applied ($\delta > 0$). The applied force to every particle is shown. The diagram shows the components of the applied force to a particle.

affect the chain reptation and thus the resulting drift velocity. We could determine distinct mechanisms responsible for the observed trends as a function of the force strength and chain length.

2. Model

The model is based on the reptation concept in which gel fibers play the role of obstacles that inhibit the lateral movement of a diffusing chain. The confinement is such that the chain moves in a tube and the dominant motion is one-dimensional. The diffusing chain, consisting of N particles, is represented by a string of beads and holes (or vacancies) and it is placed in a square lattice of constant a determined by obstacles (represented by crosses) as seen Fig. 1(a). For the sake of simplicity, we will assume that the obstacles define a square network. The chain is not allowed to cross any of the obstacles but it can move in between. The distance between two consecutive particles can be either a, $2a$, or $2^{1/2}a$ (in the last two cases there is a hole between the particles). Only loops of the string in which at least one obstacle is surrounded by the chain are allowed (hernias are not allowed). Although consecutive beads or holes cannot occupy the same site, when loops form a given lattice site can be occupied by more than one particle or hole. Each end particle has a corresponding pre-end particle, that is, the consecutive particle of this end particle along the chain.

When external forces are not applied, the jumping rules of the model are as follows (see Fig. 1(b) with $\delta = 0$).

- An end particle with a nearest site occupied by its corresponding pre-end particle jumps with a probability per unit time $p_a/3$ to each of the three nearest sites that are not occupied by the pre-end particle, see Fig. 1(b). Then, the total jumping probability per unit time is p_a. If the jump takes place, a hole is created.
- An end particle not having a nearest site occupied by its corresponding pre-end particle (i.e. there is a hole between these two particles) jumps towards the hole with a probability per unit time p_b. If the jump takes place, a hole is annihilated.
- A middle particle (particles which are not located at the end of the chain) with one of its nearest site along the chain occupied and the other one empty jumps to the hole with a probability per unit time p_c.
- A middle particle with both nearest sites along the chain occupied, or both nearest sites along the chain empty (i.e., a middle particle between two holes), does not jump and remains at its original position.

Hence, p_a, p_b, and p_c are the free parameters of the model. In the following we will use that the distance a between adjacent sites of the square lattice and the unit time are both equal to 1.

A hole is created or annihilated every time an end particle jumps moving away from the chain or towards the chain, respectively. An end particle jumping attempt that creates a hole is successful with frequency $p_a(1-P_h)$, where P_h is the hole probability. Similarly, an end particle jumping attempt that annihilates a hole succeeds with frequency p_bP_h. In equilibrium we expect the same frequency for creation and annihilation. Thus, P_h can be expressed as

$$P_h = \frac{p_a}{p_a + p_b}. \tag{1}$$

When no external forces are present, the hole probability P_h is uniform along the entire chain. Under these conditions, the average length of chains, l, is given by

$$l = N + P_h(N - 1). \tag{2}$$

If there is an applied external field, implying a force to the right, the jumping rates of a particle to the right and to the left will be considered to be $(1 + \delta)k$ and $k/(1 + \delta)$, respectively. k is the jumping frequency when no force is applied, and $\delta \geq 0$. In what follows, in a general sense, we will refer to δ as the applied force to a particle of the chain. However, the external force applied to a particle has a net component to the right of magnitude 2δ and another component upwards of the same magnitude. Thus, the net force applied to every particle is $2\sqrt{2}\delta$, see Fig. 1(b). We can also refer to the external force in terms of a dimensionless applied electric field E. Indeed, $1 + \delta = \exp(E_x/2) = \exp(E_y/2)$, where $E_x = E_y = E/\sqrt{2} = qE'_x a/kT = qE'_y a/kT$, where E'_x and E'_y are the actual electric field in the x-direction and y-direction, respectively, and q is the associated charge to every particle. To facilitate comparison with previous work, we include both manners to refer to the applied force. Note that for $\delta \ll 1$, $\delta \sim E$.

First, we will discuss some general theoretical considerations used in this work. Then, we will present the case in which the total applied force is small, i.e., $N\delta \to 0$. Next, we will analyze the results for chains of any length with $\delta \to 0$. Finally, we will discuss the results corresponding to large forces.

3. Diffusion coeficient

Using scaling arguments [7] we obtained an analytical approximation for the diffusion constant of the center of mass of the chains in two dimensions. Let us consider the case of a chain that moves in a medium with fixed obstacles that restrict the lateral motion of the chain. This situation can be approached with a chain confined in a tube. After a time, t_{esc}, the chain escapes from its original tube and adopts a new configuration that is not correlated with the initial one. In other words, at the scale of time t_{esc} the center of mass of the chain performs an ordinary random walk. Then, one can write that $r^2_{cm} \sim D_{2D}t$, where $t \geq t_{esc}$, r^2_{cm} is the mean square displacement of the center of mass and D_{2D} is the diffusion coefficient in two dimensions.

Considering now the one-dimensional motion of the chain along the tube, $l^2 \sim D_{1D}t_{esc}$, where l is the average length of the chain and D_{1D} is the diffusion constant in its tube (i.e., D_{1D} is the one-dimensional diffusion coefficient). At $t = t_{esc}$, the mean square displacement, r^2_{cm}, behaves as the square of the mean value of the end-to-end distance of a chain, r^2 $(r^2_{cm} \sim r^2)$. By combining these expressions, the diffusion constant of the center of mass of the chains behaves as

$$D_{2D} = C\left(\frac{r}{l}\right)^2 D_{1D}, \tag{3}$$

where C is a constant. The exact expression of D_{1D}, valid for $N \geq 2$, was found in Ref. [11] and it is given by

$$D_{1D} = \frac{p_a p_b p_c}{(p_a + p_b)\left[(N - 2)(p_a + p_b) + 2p_c\right]}. \tag{4}$$

When there are no external forces, $r \sim l^{1/2}$. Thus, from Eqs. (1)–(4) we can write

$$D_{2D} = A\frac{p_a p_b p_c}{\left[(N - 2)\,(p_a + p_b) + 2p_c\right]\left[N\,(p_a + p_b) + (N - 1)\,p_a\right]}, \tag{5}$$

where A is a constant. In Ref. [10] it was found that $A = 1.06$. For $p_a + p_b = p_c$, D_{2D} behaves as $1/N^2$ even for quite small values of N ($N \geq 10$). Let us note that the above arguments hold for $D \geq 2$. Then, we expect that Eq. (5) is also valid in 3D with an appropriate value of constant A.

4. Results and discussions

4.1. Small forces ($\delta \ll 1$)

4.1.1. Small total force ($N\delta \ll 1$)

In the limit of very small total force ($N\delta \ll 1$) one expects that the Einstein relation holds, then one has

$$v_{\text{drift}} = D_{2D}2\sqrt{2}N\delta, \tag{6}$$

where $2\sqrt{2}N\delta$ is the total force applied to the chain and D_{2D} is the diffusion coefficient in two dimensions. From Eqs. (5) and (6), one obtains an analytic approximation for drift velocity of the center of mass of a chain of N beads

$$v_{\text{drift}} = A\frac{p_a p_b p_c}{\left[(N - 2)\,(p_a + p_b) + 2p_c\right]\left[N\,(p_a + p_b) + (N - 1)\,p_a\right]}2\sqrt{2}N\delta. \tag{7}$$

Fig. 2 shows Monte Carlo results for the drift velocity as a function of $1/N$ and with dashed lines the analytical approximation, Eq. (7), for two values of the applied force. This approximation has been verified using Monte Carlo simulations for different values of p_a, p_b, p_c, and δ.

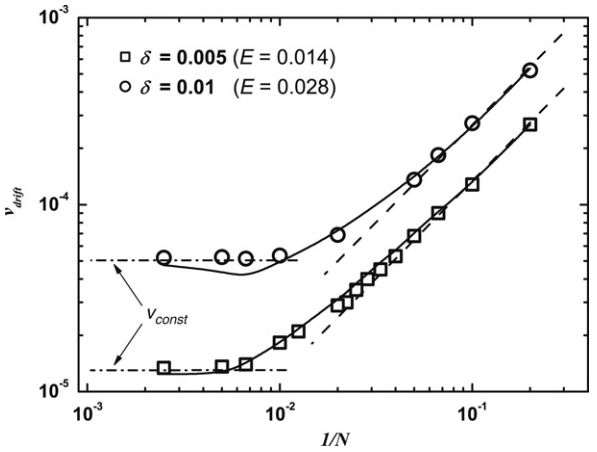

Fig. 2. Drift velocity of chains consisting of N beads for two values of the applied force δ (or field E). Dashed lines represent the approximation given by Eq. (7), which is valid for $N\delta \ll 1$. Solid lines correspond to the approximation given by Eq. (8), valid for every N and $\delta \ll 1$. Horizontal dashed-dotted lines correspond to the constant value of v_{drift} obtained for large value of N. Monte Carlo results were obtained using $p_a = p_b = 0.25$ and $p_c = 0.5$. Error bars are smaller than the symbols size.

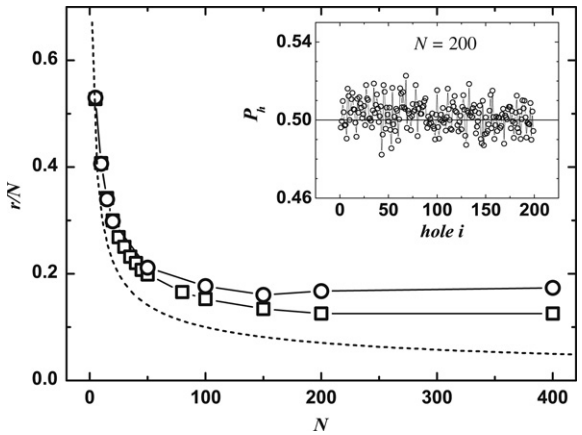

Fig. 3. Ratio r/N vs. N, where r is the mean value of the end-to-end distance of a chain of N particles. The values for the parameters of the model are $p_a = p_b = 0.25$, $p_c = 0.5$, $\delta = 0.005$ (open squares) and $\delta = 0.01$ (open circles). The dashed line indicates the behavior when no forces are present ($r \sim N^{-1/2}$). The hole probability, P_h, along the chain for $N = 200$ is shown in the inset (using $p_a = p_b = 0.25$, $p_c = 0.5$, and $\delta = 0.005$); these results were obtained averaging over 5000 samples. The horizontal line is the expected value of P_h.

4.1.2. Small forces and large chains ($\delta \ll 1, N \gg 1$)

The forces δ can produce two different kind of deformations: (a) the deformation of the tube, and (b) the deformation of the chain within the tube. In the case of $N\delta \ll 1$ both deformations are negligible and the Einstein relation holds as was above mentioned. We found that, in the case of $\delta \ll 1$ and $N \gg 1$, the tube containing the chain deforms despite the smallness of the force applied, i.e. the relation $r \sim l^{1/2}$ does not hold any longer. This can be clearly observed in Fig. 3 in which the ratio r/N becomes constant for large values of N. As in the previous case, long chains do not deform within the tube. This is verified by examining the hole distribution along the chains. As seen in the inset of Fig. 3, the hole probability P_h for a chain of $N = 200$ is the same along the chain and the average value is that of a equilibrium. Therefore, the average chain length, l, can be determined using Eq. (2). Note that $l \sim N$ for large values of N and thus, from Fig. 3, $r \sim l$.

For this regime we propose the validity of an *extended Einstein relation* equivalent to Eq. (6). By combining Eqs. (3) and (6) one obtains

$$v_{\text{drift}} = C \left(\frac{r}{l}\right)^2 D_{1D} 2\sqrt{2} N\delta. \tag{8}$$

We can determine the value of the constant C by matching this expression to Eq. (7) for small values of N. As before, the diffusion coefficient D_{1D} is given by Eq. (4) because, for $\delta \ll 1$, there is no deformation of the chain inside the tube. The values of the ratio r/l are obtained from Monte Carlo results. This means that to compute v_{drift} we need this ratio that must be obtained with numerical simulations. In Fig. 2 we show approximations given by Eq. (8) that, using the results of Fig. 3,

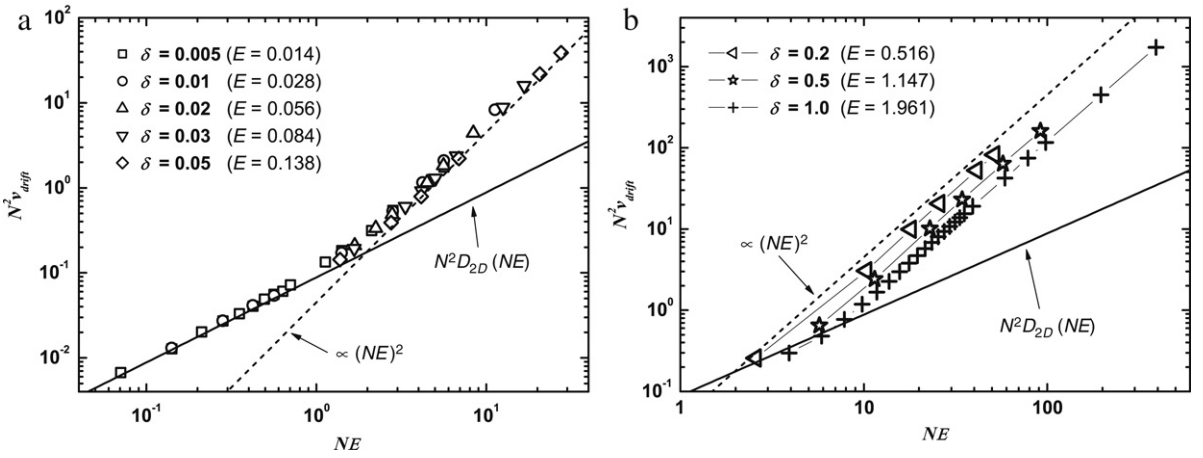

Fig. 4. Rescaled drift velocity $v_{\text{drift}}N^2$ as a function of the total force applied to the chain NE. In (a) the small forces case is shown ($\delta \ll 1$). The solid line corresponds to the re-scaled equation (7) and the dashed line indicates a behavior of the type $(NE)^2$. In (b) results corresponding to large forces applied to every particle are plotted. The solid and dashed lines are the same than in (a). In both cases, the parameters of the model are $p_a = p_b = 0.25$ and $p_c = 0.5$.

fit very well the simulations. This approximation was verified for other sets of p_a, p_b, p_c and δ, where $p_a + p_b = p_c$ with $p_a = p_b$ and $p_a \neq p_b$.

Note that in the necklace model, within some range, we can choose the average length of the chain for the same number of beads and, independently, the mobility of the end beads can be made equal to the mobility of the middle beads. This permits, [with $p_a + p_b = p_c$, see Eq. (4)] to have a curvilinear diffusivity with a dependence $1/N$ for any N, which is in agreement with the reptation theory [1,2]. In 3D, see the comment below Eq. (5), the dependence $1/N^2$ for $N \geq 10$ has been observed in entangled polymer melts for tracer diffusion [12], i.e. when obstacles can be considered to be immobile as in electrophoresis. Furthermore, with this election of parameters, external forces produce no deformation in the one-dimensional case. Indeed, in Ref. [11] we found that – in one dimension, for $p_a + p_b = p_c$ and any values of N and δ $(N \geq 2, \delta > 0)$ – the chains are dragged by external forces without any deformation (i.e.: P_h is the same along the chains). Therefore, if a deformation of the chain inside the tube appears, it must be directly related to the two dimensional motion in which new effects are present. For this reason in what follows we will use $p_a + p_b = p_c$. Furthermore, in the necklace model, deformations, which will be discussed below, can be readily evaluated through the hole distribution, and it is possible to distinguish tube deformation from chain deformation.

Fig. 4 shows rescaled drift velocities $v_{\text{drift}}\, N^2$ as a function of NE, which is proportional to the total applied force, for $p_a = p_b = 0.25$ and $p_c = 0.5$, with different values of δ. The drift velocity dependence with N when the applied force on every particle is small is shown in Fig. 4(a). Two regimes clearly emerge according to the size of the chains. For relatively short chains, when $NE \ll 1$, $v_{\text{drift}} \sim E/N$ because $D_{2D} \sim 1/N^2$, see Eqs. (5) and (6). For long chains, in which $E \ll 1$, it is found that $v_{\text{drift}} \sim E^2$. From Monte Carlo results (not shown here) we found that $(r/l)^2_{\text{const}} \sim \delta$, where $(r/l)_{\text{const}}$ is the value of r/l for $N \gg 1$, which does not depend on N (see Fig. 3). Then, from Eq. (8), the drift velocity, for $N \gg 1$ and $\delta \ll 1$, is proportional to δ^2 and independent of N, since $D_{1D} \sim 1/N$. This is in agreement with experiments of DNA migration in electrophoresis (see [13] and references there in). It is important to note that in both regimes the chain deformation within the tube is negligible. The large NE regime ($v_{\text{drift}} \sim E^2$) appears due to the tube deformation. The same types of regimes were found in the Duke model (see Refs. [6] and [13]), and in the biased reptation model that has a different dynamics (see Refs. [14] and [15]).

Fig. 2 shows that, for small δ and large enough values of N, the drift velocity takes a constant value v_{const}. This behavior corresponds to the large total force regime shown in Fig. 4(a). Strictly speaking, we do not know if the drift velocity remains constant as N goes to infinite, or v_{drift} decreases in this limit. Unfortunately, we cannot answer this question because the obtaining of v_{drift} for larger values of N is beyond our computation facilities. In other words, we do not know if there is another regime for $E \to 0$, $N \to \infty$, and $NE > 30$.

4.2. Large forces

The rescaled drift velocities $v_{\text{drift}}N^2$ as a function of the total force applied when the applied force on every particle cannot longer be considered small are shown in Fig. 4(b). The behavior is very different from what was observed for smaller applied forces. We will show that the response of the chains to large forces involves not only the deformation of the tube but of the diffusing chain itself within the tube. Moreover, we can define that the applied force is large if the chain suffers an appreciable deformation.

In Fig. 5 we can appreciate the chain deformation due to large applied forces. The chain deformation directly reflects on the hole probability along the chain that not only is not uniform but can be significantly larger than that of equilibrium, see Eq. (1). We found that the chain deformation increases with N for the same value of δ (the total force $N\delta$ increases). The

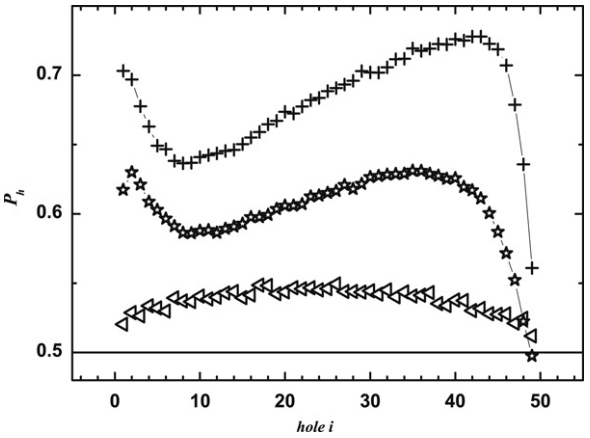

Fig. 5. Probability, P_h, for a hole between two particles along a chain with $N = 50$ in the case of large forces applied to every particle. When no forces are applied, $P_h = 0.5$ (see Eq. (5)) which correspond to the solid horizontal line. The parameters of the model are $p_a = p_b = 0.25$ and $p_c = 0.5$. Open triangles correspond to $\delta = 0.2$, open stars to $\delta = 0.5$, and crosses to $\delta = 1.0$. Chains align with the field. For $\delta = 0.2$, not a very large field, chain ends play the roles of head and tail alternatively during the simulation resulting in a symmetric hole distribution. For $\delta = 0.5$ and $\delta = 1$, one of the chain ends plays the role of head along the whole simulation.

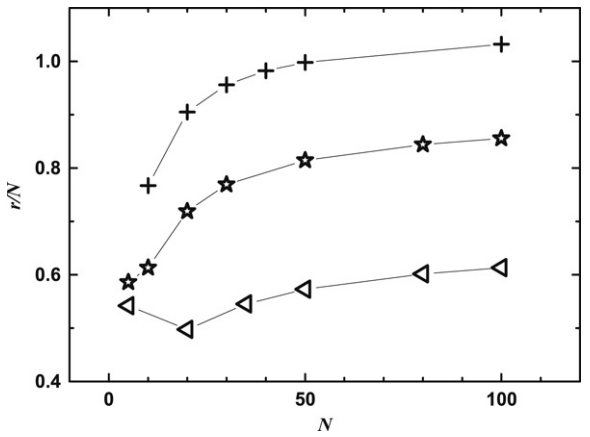

Fig. 6. Ratio r/N vs. N where r is the mean value of the end-to-end distance of a chain of N particles. The values for the parameters are $p_a = p_b = 0.25$ and $p_c = 0.5$. Open triangles correspond to $\delta = 0.2$, open stars to $\delta = 0.5$ and crosses to $\delta = 1.0$.

difference between the hole distributions of Fig. 5 and that in the inset of Fig. 3 is striking. Note that the inset of Fig. 3 shows results for $N = 200$ and Fig. 5 for $N = 50$; since deformation increases with N, longer chains are even more deformed than those of Fig. 5. Thus, we cannot longer calculate the average chain length using Eqs. (1) and (2).

It was also found that, for large forces, chains are stretched (r/N is much larger than for cases of small δ, see Figs. 3 and 6) and chains align with the field. The reported hole distributions of Fig. 5 were obtained performing the time average of one sample over a total time $T = 10^9$, averaging 10^4 configurations taken on intervals of 10^5 units of time. For $\delta = 0.2$ the chain deformation is not very pronounced and chain ends play the roles of head and tail alternatively during the simulation resulting in a symmetric hole distribution (the roles of head and tail change around 20 times during T). In the other two cases, for which $\delta = 0.5$ and $\delta = 1$, once the chain is aligned with the field, one of the chain ends plays the role of head along the whole simulation. We did not observe a chain re-orientation after the time T indicating that the probability for this event is extremely low. Note that, after this time, the chain moves by drift approximately 2.5×10^7 lattice constants for $\delta = 0.5$, more than 3×10^5 times the average chain length. Interestingly, the resulting chain deformation is not symmetric. Furthermore, we found that the ratio r/N increases with N, i.e., the distance between the chain ends increases faster than the number of particles in the chain, see Fig. 6. Of course, this cannot occur indefinitely because of the chain integrity; at some point the tube cannot longer be straighter and the ratio r/N stops increasing.

In Fig. 4(b), due to the scales used, the details in the behavior of the drift velocity as a function of the chain length cannot be appreciated. In Fig. 7 we present v_{drift} versus $1/N$ in log–log plot for a large value of the applied force ($\delta = 1$). This figure shows that for small values of N, v_{drift} decreases with N to a minimum. After that, v_{drift} increases reaching a maximum value that is due to the tube straightening or, in other words, to a longer end-to-end distance of the chain. For a window of N, longer chains move faster than short ones. This behavior has been observed experimentally (see, for example, Ref. [16]).

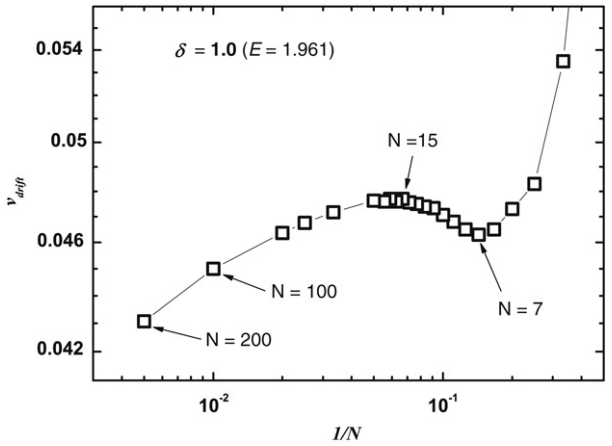

Fig. 7. Drift velocity as a function of the inverse of the number of particles of the chain for large δ in a log–log plot. Monte Carlo results where obtained using $p_a = p_b = 0.25$, $p_c = 0.5$ and $\delta = 1.0$.

We associate this phenomenon to tube straightening when the distance between the chain ends increases faster than the number of particles in the chain as shown in Fig. 6. Finally, v_{drift} decreases again, what is correlated with a noticeable chain deformation.

As commented above, for $p_a + p_b = p_c$, chains are dragged by external forces without any deformation in one dimension. Thus, chain deformation is a phenomenon that must be directly related to the two-dimensional character of the present model. The observation that the average hole probability increases (Fig. 5) indicates the presence of some regions in the chains with a mobility lower than average in such a way that the applied forces stretch the chains. This idea is that of self-trapping of Noolandi et al. [16], in which fragments of the chain stop migrating during some time as they get trapped in loop-like conformations. As a consequence, the drift velocity reduces with N as self-trapping becomes more likely. Our modeling predicts this phenomenon to take place for very large fields but, to our knowledge, experimental results have not been reported.

5. Conclusions

The characteristics of necklace model allow us to identify the effects of the forces on the chains and the resulting mechanisms that affect the drift velocity. In particular, the hole distribution along the chain and the end-to-end distance of the chain give us the information on the chain deformation within the tube and on the tube deformation, respectively.

For the chosen condition of the parameters in the model, $p_a + p_b = p_c$, the one-dimensional diffusivity is simply related to N as $D_{1D} \sim 1/N$. For small total applied forces, i.e. $N\delta \ll 1$, $r \sim l^{1/2}$ and l is proportional to N; then, v_{drift} scales as $1/N$. For small forces ($\delta \ll 1$), we propose the approximation given by Eq. (8). The v_{const} regime shown in Fig. 2 is due to the linear relation between the end-to-end distance of the chain and its chain length. Indeed, for small applied forces but large N, when the condition $N\delta \ll 1$ is not longer valid, $r/l \sim$ constant and thus v_{drift} converges to a constant value, in agreement with Monte Carlo data. In short, the behavior shown in Fig. 4(a) is due to the crossover from $r \sim l^{1/2}$ to $r \sim l$ regimes. No other effects are present in these regimes; in particular, the distribution of holes along the chain remains unaffected and is the same found when no force is applied. This is the reason why in the approach that leads to Eq. (8) we can use the same one-dimensional diffusion constant, D_{1D}, for both regimes.

For large forces, when the condition $\delta \ll 1$ does not hold, the distance between the chain ends can increase faster than the number of particles in the chain and thus the drift velocity becomes larger with N. Eventually this effect cannot occur indefinitely and the ratio r/l becomes constant again. Large forces have another effect: the chain within the tube is deformed as the hole distribution is not longer constant along the chain indicating self-trapping. Under this condition, the mobility is reduced and the drift velocity drops with N as longer chains are more and more deformed.

In the present paper only results with $p_a = p_b = 0.25$ and $p_c = 0.5$ are shown. But, the general conclusion of the present work were verified for other values of p_a, p_b and p_c, for which the relation $p_a + p_b = p_c$ hold (with $p_a = p_b$ and $p_a \neq p_b$).

In Ref. [10] we presented two versions of the necklace model, the non interactive and the self avoiding cases. In this work we focus on the non interacting case because $D_{2D} \sim 1/N^2$ as observed in experiments. Self-avoidance leads to a different N dependence, $D_{2D} \sim 1/N^{3/2}$ [10], that directly reflects on the drift velocity for small fields. Conversely, for large fields, chains are stretched, so self-avoiding chains have the same behavior than non-self avoiding ones.

Acknowledgments

This work was partially supported by the National Council for Scientific and Technical Research (CONICET) of Argentina. Two of us (G.T and H.M.) acknowledge ANPCyT (PICT 2004 No 17-20075, Argentina) for financial support.

References

[1] P.G. de Gennes, J. Chem. Phys. 55 (1971) 572.
[2] P.G. de Gennes, Scaling Concepts in Polymer Physics, Cornell University Press, Ithaca, NY, 1979.
[3] M. Doi, S.F. Edwards, The Theory of Polymers Dynamics, Clarendon Press, Oxford, 1986.
[4] J.L. Viovy, Rev. Modern Phys. 72 (2000) 813.
[5] M. Rubinstein, Phys. Rev. Lett. 59 (1987) 1946.
[6] T.A.J. Duke, Phys. Rev. Lett. 62 (1989) 2877.
[7] B. Widom, Physica A 236 (1997) 1.
[8] S.E. Guidoni, H.O. Mártin, C.M. Aldao, Eur. Phys. J. E 7 (2002) 291.
[9] S.E. Guidoni, H.O. Mártin, C.M. Aldao, Phys. Rev. E 67 (2003) 031804.
[10] G. Terranova, C.M. Aldao, H.O. Mártin, Phys. Rev. E 76 (2007) 031111.
[11] G. Terranova, H.O. Mártin, C.M. Aldao, Phys. Rev. E 72 (2005) 061108.
[12] C.Y. Liu, R. Keunings, C. Bailly, Phys. Rev. Lett. 97 (2006) 246001.
[13] G.T. Barkema, F. Marko, B. Widom, Phys. Rev. E 49 (1994) 5303.
[14] G.W. Slater, J. Noolandi, Phys. Rev. Lett. 55 (1985) 1579.
[15] T.A.J. Duke, A.N. Semenov, J.L. Viovy, Phys. Rev. Lett. 69 (1989) 3260.
[16] J. Noolandi, J. Rousseau, G.W. Slater, C. Turmel, M. Lalande, Phys. Rev. Lett. 58 (1987) 2428.